FINITE-ELEMENT ANALYSIS OF CONCRETE SLABS AND ITS IMPLICATIONS FOR RIGID PAVEMENT DESIGN

Y. H. Huang and S. T. Wang, Department of Civil Engineering,
University of Kentucky

A finite-element method programmed for a high-speed computer was developed for determining the stresses in concrete slabs with load transfer at the transverse joints. The method is based on the classical theory of thin plates on Winkler foundations and yields numerical results that check closely with other available solutions as well as with the experimental measurements from the AASHO Road Test. Although a single value of the modulus of subgrade reaction can be selected to predict approximately the stresses for various slab thicknesses and axle loads, it was found that, under a given axle load, a better agreement between theoretical and experimental results could be obtained if greater subgrade moduli were used for thicker pavements, a fact contributing to the nonlinear behavior of subgrade soils. Numerical results are presented to illustrate the effect of loading position, load transfer, and loss of subgrade contact on critical stresses in rigid pavements. When load transfer is provided at the transverse joint, the most critical stress in highway pavements occurs when the load is near the edge and far from the joint. It is suggested that the edge stress, instead of the stress at the joint, be used for the design of highway pavements.

•THE determination of stresses due to wheel loads in concrete pavements has been a subject of major concern for more than four decades. In 1926 Westergaard (1), using the theory of elasticity by assuming the subgrade as a Winkler foundation, developed a mathematical method for determining the critical stresses in concrete highway pavements resulting from three cases of loading: load applied near the corner of a large slab, load applied near the edge of a large slab but at a considerable distance from any corner, and load applied at the interior of a large slab at a considerable distance from any edge. In extending the method to airport pavements, he later developed new formulas (2, 3) that give the stresses and deflections at an edge point far from any corner and at an interior point far from any edge. These formulas were then employed by Picket and Ray (4) for developing influence charts, which have been used by the Portland Cement Association (5, 6) for the design of highway and airport pavements.

In comparing the critical corner stress obtained from Westergaard's formula with that from field measurements, Pickett found that Westergaard's corner formula, based on the assumption that the slab and subgrade were in full contact, always yielded a stress that was too small. By assuming that part of the slab was not in contact with the subgrade, he developed a semi-empirical formula that was in good agreement with both theoretical and experimental results. Pickett's corner formula, with a 20 percent allowance for load transfer, was used previously by the Portland Cement Association (7) for the design of highway pavements.

All the preceding theoretical solutions are based on an infinitely large slab, with a load at the corner, on the edge, or in the interior, and therefore may not be applicable to today's 12-ft wide lanes with most traffic moving at some distance from slab edges

Publication of this paper sponsored by Committee on Rigid Pavement Design.

and corners. With the advent of high-speed computers and the powerful finite-element method, it is now possible to analyze rectangular slabs subjected to any wheel loads and boundary conditions. The purposes of this paper are (a) to present a finite element method programmed for a high-speed computer for determining the stress distribution in a rectangular concrete slab, with or without load transfer at the transverse joint; (b) to compare the results of the finite-element method with other theoretical solutions available as well as with the experimental measurements from the AASHO Road Test, so as to check the accuracy and validity of the method; and (c) to investigate the effect of loading position, load transfer, and loss of subgrade contact on the critical stress in some typical pavements, so as to shed light on current concepts of rigid pavement design.

The finite-element method presented here is quite different from the discrete-element method employed earlier by Hudson and Matlock (8) and later by Vesic and Saxena (9) for the analysis of concrete pavements. The discrete-element method is more or less similar to the finite difference method by considering the slab as an assemblage of elastic joints, rigid bars, and torsional bars. The finite-element method is based on the theory of minimum potential energy by dividing the slab into small elements interconnected only at a finite number of nodal points. The major advantages of the finite-element method are that elements of varying sizes can be easily incorporated in the analysis and that no special treatment is needed at a free edge. As a result, the finite-element method generally yields a stiffness matrix that is symmetric, positive, and definite, and the large number of simultaneous equations can be solved by an effective scheme, although this symmetric characteristic was not fully utilized in this study because of the assumption of load transfer at the joint.

DESCRIPTION OF METHOD

The finite-element method employed in this study is based on the classical theory of thin plates by assuming that the plane before bending remains plane after bending. In addition to the basic requirements that the slabs are homogeneous, isotropic, and elastic, it is further assumed that the subgrade acts as a Winkler foundation; i.e., the reactive pressure between subgrade and slab at any given point is proportional to the deflection at that point. The procedure follows essentially that of Zienkiewicz and Cheung (10, 11) and will not be presented here. Only the general approach, the treatment of doweled joints, and the capability of the computer program will be briefly described.

General Approach

Figure 1 shows a rectangular finite element with nodes i, j, k, and l. At each node, there are three fictitious forces and three corresponding displacements. The three forces are a vertical force, F_w; a couple about the x-axis, $F_{\theta x}$; and a couple about the y-axis, $F_{\theta y}$. The three displacements are the deflection in the z-direction, w; a rotation about the x-axis, θ_x; and a rotation about the y-axis, θ_y. These forces and displacements are related by

$$\begin{Bmatrix} F_i \\ F_j \\ F_k \\ F_l \end{Bmatrix} = [K] \begin{Bmatrix} \delta_i \\ \delta_j \\ \delta_k \\ \delta_l \end{Bmatrix} + kab \begin{Bmatrix} \delta'_i \\ \delta'_j \\ \delta'_k \\ \delta'_l \end{Bmatrix} \tag{1}$$

in which [K] = stiffness matrix, the coefficients of which depend on the dimensions, a and b, of the element and the Young's modulus and Poisson's ratio of the slab; k = modulus of subgrade reaction; and at any given node i is

$$F_i = \begin{Bmatrix} F_{wi} \\ F_{\theta xi} \\ F_{\theta xi} \end{Bmatrix}, \quad \delta_i = \begin{Bmatrix} w_i \\ \theta_{xi} \\ \theta_{yi} \end{Bmatrix}, \quad \delta'_i = \begin{Bmatrix} w_i \\ 0 \\ 0 \end{Bmatrix}$$

The stiffness matrix for a rectangular element was tabulated by Zienkiewicz and Cheung (10) and is used in the present analysis. By superimposing the stiffness matrices over all elements and replacing the fictitious nodal forces with the statistical equivalent of the externally applied loads, a set of simultaneous equations was obtained for solving the unknown nodal displacements. The nodal moments and stresses were then computed from the nodal displacements, using the stress matrix tabulated by Zienkiewicz and Cheung (10). Because the stresses at a given node computed by means of one element might be different from that by the neighboring elements, the stresses in all adjoining elements were computed and their average values obtained.

Doweled Joints

The finite-element analysis of concrete slabs with doweled joints as developed here is believed to be original and provides an effective method for solving this complex problem. Figure 2 shows a load applied on the left slab of a two-slab system connected by dowel bars at the joint. If no dowels are provided at the joint, each slab will act independently, and it is only necessary to consider the left slab. When dowels are provided, part of the wheel load will be transferred from the left slab to the right slab. The efficiency of load transfer can be defined as

$$L = \frac{w_r}{w_l} \times 100 \qquad (2)$$

in which L = efficiency of load transfer, w_l = deflection of the left or loaded slab at the joint, and w_r = deflection of the right or unloaded slab at the joint. When no dowels are used, $w_r = 0$, and the efficiency of load transfer is zero. When $w_l = w_r$, or both slabs deflect the same amount at the joint, the efficiency of load transfer is 100 percent.

For the ease of explanation, each slab is divided into two elements (Fig. 2). There are a total of 12 nodes, each having three unknown displacements, or a total of 36 equations. These equations can be obtained by first assuming the discontinuity of the two slabs at the joint, so neither moment nor shear can be transferred through the joint. For example, let us look at the three equations at node 4. The 10th equation gives the vertical force, the 11th equation gives the couple about the x-axis, and the 12th equation gives the couple about the y-axis. The corresponding equations at node 7 are the 19th equation for the vertical force, the 20th equation for the couple about the x-axis, and the 21st equation for the couple about the y-axis. Because dowel bars cannot transmit moments from one slab to the other, the addition of the dowel bars will make no change in the 11th, 12th, 20th, and 21st equations. However, because of the transfer of shear, the sum of the vertical forces given by the 10th and 19th equations must be equated to the external force applied at node 4. In other words, the 10th and 19th equations are combined to form a new equation replacing the original 10th equation. The original 19th equation is then replaced by Eq. 2, which is written as

$$w_4 = \frac{100}{L} w_7 \qquad (3)$$

Because two original equations are replaced by two new equations, the total number of equations remains unchanged. The same procedure can be applied to nodes 5 and 8 as well as nodes 6 and 9. This modification destroys the symmetry of the stiffness matrix and results in an upper half band being greater than the lower half, so both the upper and lower bands must be stored. The Gauss elimination method with banded matrix provided by the IBM scientific subroutine package was used in this study to solve the simultaneous equations.

Computer Program

A general computer program was developed for determining the stresses in a pavement system composed of a series of up to three slabs connected by dowels at the transverse joints. The three slabs are used because this is a general case with the

loads applied on the middle slab, which is connected at each end to a neighboring slab by dowel bars. The use of more than three slabs is not necessary because the additional slabs are far from the load and have practically no effect on the stresses in the loaded slab. When the loads are applied near the transverse joint, only two slabs are generally sufficient, and the slab at the far end can be ignored.

Figure 3 shows the finite-element network of a three-slab system under a single- or tandem-axle load, which will be subjected to later analysis. The input parameters, which control the size and division of the slabs in this case, are number of slabs = 3; number of y-coordinates = 7; number of x-coordinates for slab 1 = 4; number of x-coordinates for slab 2 = 7; number of x-coordinates for slab 3 = 4; y-coordinates = 0, 17, 34, 57, 80, 105, and 144 in.; x-coordinates = 0, 70, 130, 180, 180, 232, 256.5, 281, 305.5, 330, 360, 360, 400, 470, and 540 in. The same program can be used for two slabs by setting the number of horizontal coordinates for slab 1 to 0, and for one slab by setting the number of horizontal coordinates for both slab 1 and slab 3 to 0; the horizontal coordinates must also be changed accordingly.

The tire imprints are converted to rectangular areas, and the coordinates of their sides must be given, so that the program can distribute the wheel loads among adjacent nodes by statics (10, 11). The program can compute several different loadings at the same time. The additional computer time due to these additional loads is very small because Gauss elimination of the coefficient matrix is carried out only once regardless of the number of loads involved.

If the problem to be solved exhibits symmetry with respect to one or both axes, it is only necessary to consider one-half or one-quarter of the pavements, which saves a great deal of computer time.

The program can be used to investigate the effect of partial subgrade contact on stress distribution. The nodal numbers at which subgrade reaction resulting from loss of subgrade contact does not exist can be assigned, and the second term on the right side of Eq. 1 will be automatically eliminated at these nodal points when forming the simultaneous equations.

The program was written in FORTRAN IV for the IBM 360 computer, Model 65, available at the University of Kentucky.

COMPARISON WITH AVAILABLE SOLUTIONS

To check the accuracy of the finite-element method and the correctness of the computer program, it is desirable to compare the finite-element solutions with other theoretical solutions available, especially with those involving discontinuities such as the stress at the free edge of a slab. Westergaard's original work and Pickett and Ray's influence charts can be used for such purposes. Because these available solutions are based on an infinite slab, a very large slab was used in the finite-element analysis.

Westergaard's Solutions

The finite-element solutions were obtained by using a large slab, 20ℓ long by 10ℓ wide, where ℓ is the radius of relative stiffness. Because the problem is symmetrical with respect to the y-axis, only one-half of the slab was considered. The slab was divided into rectangular finite elements as shown in Figure 4. The x-coordinates are 0, $\pi\ell/8$, $\pi\ell/4$, $\pi\ell/2$, $\pi\ell$, 5ℓ, 7ℓ, and 10ℓ, and the y-coordinates are 0, $\pi\ell/4$, $\pi\ell/2$, $\pi\ell$, $1.5\,\pi\ell$, $2\,\pi\ell$, $2.5\,\pi\ell$, and 10ℓ. The Poisson's ratio of the concrete is 0.25, as was assumed by Westergaard.

Figure 4 shows a comparison between Westergaard's exact solutions for an infinite slab with a concentrated load, P, on one edge far from any corner, as indicated by the solid curves, and the finite-element solutions, as indicated by the small circles. The moment, M, and deflection, w, along the edge of slab and the deflection at a distance of $\pi\ell/4$ and $\pi\ell/2$ from the edge are presented. It can be seen that the finite-element solutions check very closely with Westergaard's results, thus indicating the accuracy of the authors' finite-element formulation.

Figure 1. Rectangular plate element.

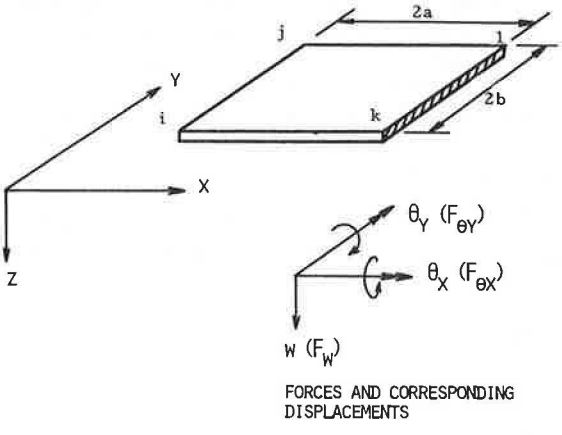

Figure 2. Two-slab system with doweled joint.

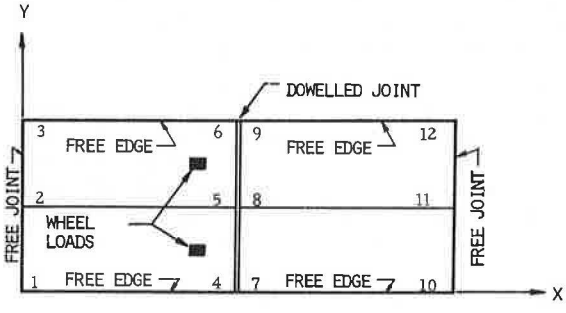

Figure 3. Three-slab system with doweled joints.

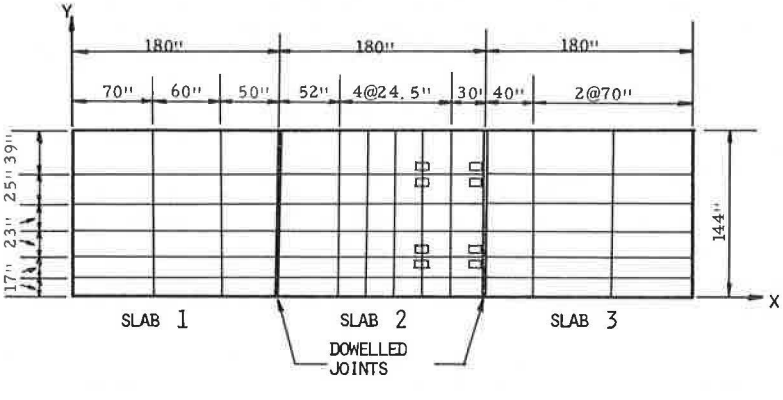

PCA's Solutions

The Portland Cement Association has made use of the influence chart developed by Pickett and Ray (4) for determining the stress on a pavement edge due to tire loads. Figure 5 (12) shows the application of the chart for determining the moment at point 0 under a 36-kip tandem-axle load having an 11.5-in. dual-tire spacing, a 49-in. tandem-axle spacing, and a 71-in. spacing between the centers of the two sets of dual tires. The load on each tire is 4,500 lb. The actual contact area is 67 in.^{2}, consisting of a rectangle with two rounded ends, but was converted to a rectangle of 6.79 by 9.87 in. The Poisson's ratio of the concrete is 0.15.

The moment, M, at point 0 in Figure 5 (due to each of the tire loads) can be determined from the number of blocks enclosed by each tire imprint, tabulated as N-counts in the figure, by

$$M = \frac{q\,\ell^2\,N}{10{,}000} \tag{4}$$

in which q = contact pressure = 67.2 psi and ℓ = 50 in. As tire 1 yields the same moment as tire 2 and tire 5 the same as tire 6, there are actually six different tire positions, some close to point 0 and some far from it, which can be used for comparison.

In the finite-element analysis, only one-half of the slab was considered because the problem could be made symmetric by placing an image tire on the left corresponding to each tire on the right. The moment thus determined was divided by two to give the moment resulting from one tire only. The horizontal and vertical coordinates for finite-element subdivisions were 0, 24, 48, 72, 96, 128, 160, 208, and 300 in.

Table 1 gives a comparison of the moments at point 0 due to six different tire positions. It can be seen that the finite-element solutions check quite well with the influence chart solution, especially when the tire is close to point 0. The large discrepancy for tire 7 is due to the fact that this tire straddles between positive and negative blocks and covers only two blocks. The percentage of discrepancy would become zero if the block enclosed was counted as 1.2 instead of the two blocks counted by the PCA.

COMPARISON WITH AASHO ROAD TEST

Although the finite-element solutions check very closely with other available solutions, the comparison is based on a large slab with free edges. Because no theoretical solutions are available for rectangular slabs with load transfer at the joint, it is desirable to compare the finite-element solutions with experimental measurements so that the validity of the method as applied to actual pavements with doweled joints can be tested. The results of the stress measurements from the AASHO Road Test (13) provide an excellent opportunity for making such comparisons.

In the AASHO Road Test, two series of experiments were made to measure the stresses in concrete slabs. The first was conducted on the main traffic loops where the stress due to moving traffic was measured at a single point on the pavement edge far from any joint. The second was conducted on the nontraffic loop where the stresses due to a rapidly oscillating load were measured at 15 different points distributed over a 6- by 6-ft area at one corner. The length of slabs consisted of 15-ft nonreinforced sections and 40-ft reinforced sections. It was found that reinforcing, or slab length, had very little effect on the stresses measured, so only the 15-ft slab was employed in the finite-element analysis.

The slabs were 15 ft long and 12 ft wide with dowels at the transverse joints and tie bars at the longitudinal joint. Because the dowels were much larger bars spaced at 12 in. in centers and the tie bars were smaller and spaced at 30 in. apart, it was assumed in the finite-element analysis that the efficiency of load transfer was 100 percent at the transverse joint and 0 percent at the longitudinal joint, or the longitudinal joint was treated as a free edge.

In computing theoretical stresses, it is necessary to know the Young's modulus and the Poisson's ratio of concrete and the modulus of subgrade reaction, k. The Young's moduli of concrete, as measured at the AASHO Road Test, were 6.25×10^6 psi for dy-

Figure 4. Comparison of finite-element solution with Westergaard's exact solution.

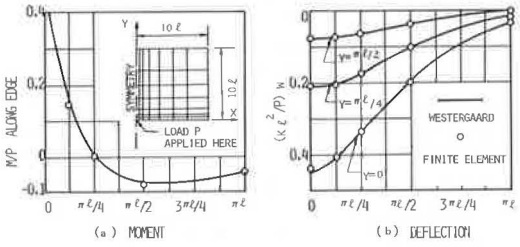

Figure 5. Contact imprints on influence chart and corresponding N-count.

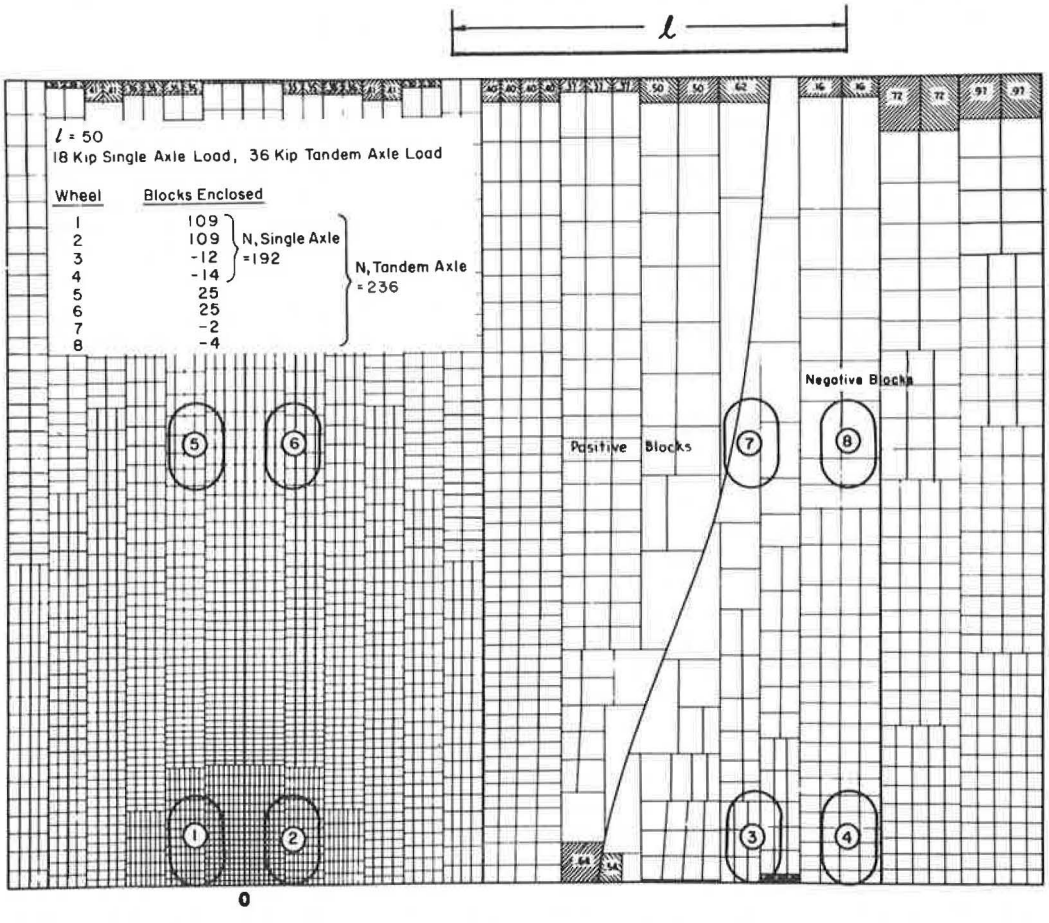

namic loads and 5.25×10^6 psi for static loads, and the Poisson's ratio was found to be 0.28. Because the type of loading does not have significant effect on the Young's modulus, a dynamic modulus of 6.25×10^6 psi was used in the finite-element analysis as well as in the conversion from the measured strains to stresses.

The determination of the subgrade k-values is much more difficult because they change appreciably with the time of the year and the type of loading. The k-values on the subbase obtained by the plate bearing test at the AASHO Road Test varied from 85 to 135 lb/in.^{3}, but these were measured during the spring when the subgrade was weak and by static or gradually applied loads. Because the stresses were measured at the AASHO Road Test mostly during the summer and fall and under dynamic or vibratory loads, larger k-values should be used.

In comparing theoretical stresses with the results of the AASHO Road Test, Vesic and Saxena (9) indicated that the k-values should be inversely proportional to the thickness of the slab and suggested the use of 90.4 lb/in.^{3} for a 5-in. slab, 47.5 lb/in.^{3} for a 9.5-in. slab, and 36.2 lb/in.^{3} for a 12.5-in. slab. These k-values are too small for the reasons discussed previously. If these values are used in the finite-element analysis, the results do not check with the test data, as will be illustrated later.

Dynamic Edge Stress

In the AASHO Road Test, the dynamic strain at the edge of pavement 7.5 ft from the joint was measured under various single- and tandem-axle loads, moving mostly at 5 mph with the center of the dual at a distance of 20 in. from the pavement edge. Statistical equations were developed by the Highway Research Board (13) to predict the dynamic edge strains for various axle loads, slab thicknesses, and temperature gradients. These strains can be converted to stresses using a dynamic Young's modulus of 6.25×10^6 psi as determined from the AASHO Road Test.

The finite-element network is shown in Figure 6. Because of symmetry, only one-half of the pavement was considered. The x-coordinates for the finite-element grid were 0, 30, 60, 90, 130, 190 and 270 in.; the y-coordinates were 0, 20, 40, 70, 90, 110, and 144 in.

Figure 6 shows a comparison of the edge stress when the temperature in the slab is uniform or the temperature gradient is zero. It can be seen that the experimental measurements (as indicated by the solid curves) check reasonably well with the finite-element solutions (as indicated by the dotted curves) for a variety of loads and slab thicknesses when a k-value of 300 lb/in.^{3} is assumed. Nearly in every case, the experimental curves have a steeper slope than the theoretical curves. The curves can be made more compatible by increasing the stress in thinner slabs by decreasing the k-value, or by decreasing the stress in thicker slabs by increasing the k-value. In other words, the k-values should increase with the increase in slab thickness. This is in contradiction to the contention by Vesic and Saxena (9) that the k-values to be used should increase with the decrease in slab thickness. Their conclusion is valid only when the subgrade soils are linearly elastic. In order to obtain solutions based on Winkler foundation comparable to those based on elastic solid, we must increase the k-value with decreasing thickness. However, because the subgrade soils are not linearly elastic and are much stiffer under small stresses and deflections, it is not difficult to explain why under a given load the k-value should increase with the increase in thickness.

The selection of a k-value of 300 lb/in.^{3} needs explanation. This value appears quite reasonable for the conditions of the subgrade and subbase and the types of loading available at the AASHO Road Test. It is well known that the stress in concrete slabs depends on the radius of relative stiffness, ℓ, which is a function of the ratio between Young's modulus of concrete and the k-value of the subgrade. If a k-value of 300 lb/in.^{3} is considered too high, it is quite possible that a Young's modulus of 6.25×10^6 psi is also too high. Thus, the same stress would be obtained if both were reduced proportionately. In fact, the k-value is a fictitious parameter not characteristic of soil behavior. If a k-value that gives a good prediction of the stress for various axle loads and slab thicknesses can be found, it is a most reasonable value to be used. Fortunately,

the value of k does not have a large effect on the computed stress. If a smaller k-value were used, the finite-element solutions, as indicated by the dotted curves, would move slightly upward, but the general trend still remains the same.

Stress Distribution Under Vibratory Loads

In the AASHO Road Test, a rapidly oscillating load at a frequency of 6 cps was applied to the pavement through two wooden pads, each having 11- by 14-in. area and spaced on 6-ft centers. The center of the outer pad was placed 1 ft from the pavement edge, thus simulating a single-axle load in the traffic loops. The major and minor principal strains at 15 points, distributed over a 36-ft^2 region bounded by the pavement edge and a transverse joint, were determined. These strains were then converted to principal stresses, and graphs of the major and minor principal stresses were published by the Highway Research Board (13).

Four loading positions were employed, with the center of the load at a distance of 0.5, 2, 4, and 6 ft from the transverse joint. The loading position, the location of points at which stresses were measured, and the finite-element subdivisions are shown in Figure 7. Because the slab on the left of the loaded slab has very little effect on stress distribution, only two slabs were considered with 100 percent load transfer at the transverse joint and 0 percent at the longitudinal joint. A k-value of 900 lb/in.^{3}, which is three times greater than the 300 lb/in.^{3} used previously for computing the edge strain, was assumed because the vibratory load was applied at a frequency of 6 cps, which is much faster than the vehicle speed of 5 mph.

Figure 8 shows a comparison of principal stresses for three cases: a 5-in. slab with 12,000-lb axle load, 9.5-in. slab with 22,400-lb axle load, and 12.5-in. slab with 30,000-lb axle load. In line with the sign convention used in the finite-element analysis, the stress is considered positive when the surface is in compression and negative when in tension, which is opposite to the sign convention reported by the Highway Research Board (13). The finite-element solutions are indicated by the solid lines for the major principal stresses and dotted lines for the minor principal stresses. The experimental data, which were obtained from the graphs of major and minor principal stresses published by the Highway Research Board, are indicated by the small circles. For loading position 1, the stresses are those along the joint. For other loading positions, they are under the respective axle at various distances from the edge.

Figure 8 shows that the finite-element solutions check quite well with the experimental measurements, except for the minor principal stress in the 5- and 9.5-in. slabs. Although it is possible to improve the agreement between theoretical and experimental data for loading position 1 by decreasing the efficiency of load transfer for the 5-in. slab to 40 percent and the 9.5-in. slab to 50 percent, these corrections do not improve significantly the situation for other loading positions. It is believed that these discrepancies are due to the curling of slabs because the experimental data were taken during the early morning hours when the corners and edges of the slab were curled upward and part of the slab is not in contact with the subgrade. Even if this curling effect were not considered, the agreement in stress distribution between theoretical and experimental data is certainly surprising and clearly indicates the applicability of the method for predicting the stresses in concrete pavements.

A k-value of 900 lb/in.^{3} seems rather large and falls outside the range recommended for use in practical design. However, if the concrete has a Young's modulus of 6.25×10^6 psi, as determined at the AASHO Road Test, the only way to make the theoretical and experimental results comparable is by the use of a large k-value. The solutions presented are certainly correct as can be proved by using the influence chart shown in Figure 5 for loading position 4, which is quite far away from the joint. For example, let us work with the 9.5-in. pavement. For a k-value of 900 lb/in.^{3}, the maximum stress on pavement edge determined from the influence chart is 183 psi, which checks with the 182 psi obtained by the finite-element method, even though the former assumes a Poisson's ratio of 0.15 and the latter 0.28. If a k-value of 47.5 lb/in.^{3}, as suggested by Vesic and Saxena (9), is used, the stress obtained from the influence chart is 332 psi, which is much greater than the observed stress of 181 psi. It appears that

Table 1. Comparison of moments.

Tire Number	Moment (in.-lb) By Influence Chart	By Finite-Element Method	Percentage of Discrepancy
2	1,831	1,861	+1.6
3	-202	-204	+1.0
4	-235	-260	+10.6
6	420	393	-6.4
7	-33	-20	-39.4
8	-67	-73	+9.0

Figure 6. Comparison of theoretical and experimental stresses at pavement edge.

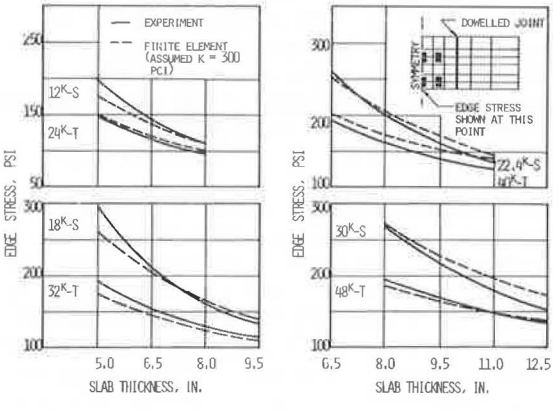

Figure 7. Loading positions and finite-element grid.

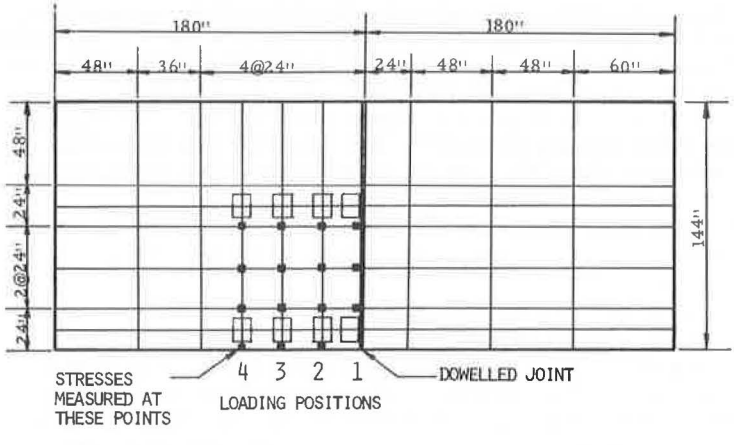

under a vibratory load the use of 900 lb/in.^{3} for k-value is more reasonable than that of 47.5 lb/in.^{3}. However, it should be reiterated that the exact value of k is not important; the most important question is whether a k-value can be found that gives a good prediction on the stress distribution for various axle loads and slab thicknesses. This study clearly shows that such a k-value does exist and that the finite-element method presented here gives a reasonable prediction of the stress distribution in concrete pavements.

IMPLICATIONS FOR PAVEMENT DESIGN

The computer program developed in this study is very effective in solving stresses in concrete pavements. Results accurate enough for design purposes can be obtained even if a coarse network is used. For the system shown in Figure 3, it took only 20 sec of compiling time and 1 min of execution time to calculate the stresses at various nodal points under 16 different loading positions. By running the program on some typical cases, interesting conclusions, which may or may not be in agreement with current design concepts, were obtained.

Critical Loading for Airport Pavements

The design method for airport pavements as developed by PCA (6) is based on interior loads because it is considered that the most critical stress in a slab occurs when the load is in the interior of the slab rather than at the doweled joint. The computer program can be used to determine how much greater the stress at the interior will be as compared to the stress at the joint. For example let us use a 12.5-in. slab with a Young's modulus of 4×10^6 psi, a Poisson's ratio of 0.15, a subgrade k-value of 100 lb/in.^{3}, and a single wheel load of 40,000 lb applied over a rectangular area 11.74 by 17.04 in. If the load is applied at the center of a 15- by 15-ft slab with a given efficiency of load transfer at two opposite joints, the maximum interior stress will be 332 psi for 100 percent efficiency, 331 psi for 80 percent efficiency, and 320 psi for 0 efficiency. If the load is applied adjacent to the joint midway between two corners, the maximum stress at the joint will be 289 psi for 100 percent efficiency, 323 psi for 80 percent efficiency, and 600 psi for 0 efficiency. This indicates that the efficiency of load transfer has relatively small effect on the interior stress but a large effect on the stress at the joint. The stress at the joint can be kept smaller than that in the interior by installing a very effective load transfer device, (e.g., one more than 70 percent efficient). Teller and Sutherland (14) investigated the efficiency of various joints and found that in many cases the deflections at the joint for both the loaded and the unloaded slabs were equal, thus indicating that this efficiency could be easily obtained in the field.

Critical Loading for Highway Pavements

In view of the fact that, on modern pavements with 12-ft lanes, traffic has moved inward from outside corners and edges, PCA (5, 12) has discontinued the use of the corner formula for pavement design. With the outer face of the exterior tire mostly about 2 ft from the pavement edge, PCA indicated that the most critical loading position was at the transverse joint, and design curves based on the influence charts shown in Figure 5 were developed for determining the maximum stress at the joint. PCA's conclusion was based on two simplifying assumptions: There is no load transfer at the joint, and the load is applied far from the corners, so that the influence chart for an infinite slab applies. Both assumptions yield a stress at the joint, as determined by the PCA method, considerably greater than the actual stress. The negligence of load transfer for highway pavements is inconsistent with PCA design method for airport pavements, which relies heavily on the load transfer at the joint. The following example illustrates the effect of loading positions on the critical stress.

Let us use a concrete pavement having a thickness of 7 in., a Young's modulus of 4×10^6 psi, a Poisson's ratio of 0.15, and a subgrade k-value of 100 lb/in.^{3}. The pavement is subjected to a typical 18-kip single-axle load and a 36-kip tandem-axle load.

According to PCA (12), the most critical stress occurs when the load is at the transverse joint and is 285 psi for single axle and 336 psi for tandem axle. The pavement was subjected to finite-element analysis using the finite-element network shown in Figure 3. The center of the outer dual is 34 in. from the edge, or the face of the tire 2 ft from the edge. The load moves from left to right, and the maximum major and minor principal stresses, when the single axle (or the front axle of the tandem) is at various distances from the joint, are given in Table 2. The efficiencies of load transfer for the two extreme cases of 0 and 100 percent are assumed. It can be seen that, if no load transfer is provided, the most critical stress takes place when the load is nearest the transverse joint. However, the computed stresses of 221 psi for single axle and 230 psi for tandem axle are much smaller than the 285 and 336 psi computed by PCA, as a direct result of PCA's assumption that the slab is infinitely wide and the load is far from the corner. If complete load transfer is provided, the most critical stress occurs when the load is at a considerable distance from the joint. The critical stresses of 225 psi for single axle and 207 psi for tandem axle are also smaller than those by PCA. The smaller stress under the tandem-axle load is caused by the compensative effect of the two axles. The actual stress of only 104 psi at the joint with 100 percent load transfer under the 18-kip single-axle load is far below the 285 psi by PCA.

The preceding discussion should not be interpreted that the current PCA method gives a design that is too conservative because there are other factors that may cause an increase in stress. The exterior tire may be closer to the pavement edge than the 2 ft assumed in the finite-element analysis. Pumping of the subgrade, blowing of the subbase, and curling of the slab may result in the loss of subgrade contact. It will therefore be interesting to investigate these extreme cases and compare the critical stresses with those by PCA.

Loss of Subgrade Contact

It is well known that concrete slabs are curled upward in early morning when the top of the slab is colder than the bottom, thus resulting in unsupported edges and corners. Loss of subgrade support may also be caused by pumping and blowing. If the conditions of contact at various points are known, the stresses in the slabs can be determined by the finite-element analysis using a method of successive approximations. However, for a qualitative comparison of critical stresses between full and partial contact, it is assumed that the two rows of nodes (Fig. 3), one on and the other next to the pavement edge, are not in contact with the subgrade; therefore, the reactive pressure at these points can be neglected.

Table 3 gives the effect of subgrade contact on critical stresses in the extreme case when the outer face of the tire is adjacent to the pavement edge. It was found that the maximum major principal stress always occurs when the load is far from the joint, whereas the maximum minor principal stress always occurs when the load is at the joint. Note that, when the pavement and subgrade are in full contact, the maximum major principal stress is always greater than the maximum minor principal stress, indicating that the critical stress occurs when the load is far from the joint. The critical stress of 391 psi for single axle is much greater than the 285 psi by PCA, whereas that of 343 psi for tandem axle is only slightly greater than the 336 psi by PCA. When the outside edge of pavement is not in contact with the subgrade, the critical stresses increase considerably, especially the minor principal stresses; however, the most critical stress still occurs when the load is far from the joint, except in the case of the tandem-axle load when no load transfer is provided.

It can be seen that, when the outer tire is nearest the pavement edge and the edge is not in contact with the subgrade, the critical stresses obtained by the finite-element method are much greater than those by PCA. Because most traffic does not travel near to the edge, except on modern freeways in urban areas, the actual stress should be much smaller. To avoid the difficulty involved in evaluating the loss of subgrade contact, it is suggested that full contact be assumed in the design of pavements. However, the assumed position of the outer tire should vary with the lane width and the type of highways and be closer to the pavement edge than anticipated to take into account the additional stress due to curling and the loss of subgrade contact.

Figure 8. Comparison of theoretical and experimental distribution of major and minor principal stresses.

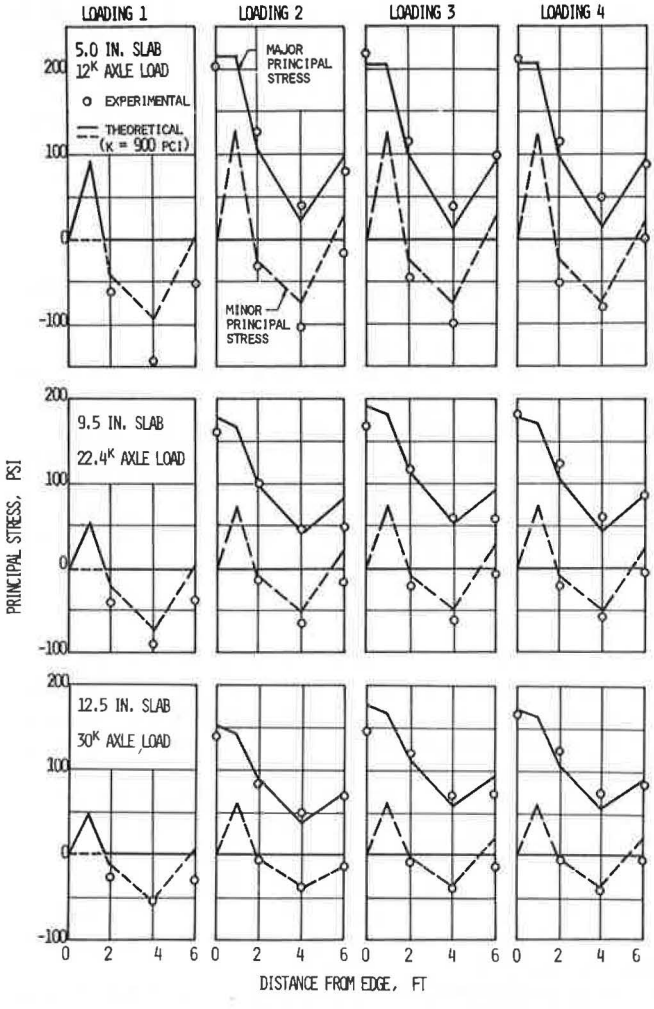

Table 2. Critical stresses with outer tire 2 ft from edge.

Distance From Axle to Joint (in.)	18-Kip Single Axle				36-Kip Tandem Axle			
	0 Percent Load Transfer		100 Percent Load Transfer		0 Percent Load Transfer		100 Percent Load Transfer	
	Major (psi)	Minor (psi)	Major (psi)	Minor (psi)	Major (psi)	Minor (psi)	Major (psi)	Minor (psi)
79	220	-27	218	-29	189	-21	192	-26
54.5	211	-37	225[a]	-40	198	-21	207[a]	-23
30	150	-54	200	-37	166	-57	197	-59
5.7	221[a]	-152	104	-66	230[a]	-121	160	-54

[a]Most critical stress for each case.

Table 3. Effect of subgrade contact on critical stresses.

Condition of Contact	18-Kip Single Axle				36-Kip Tandem Axle			
	0 Percent Load Transfer		100 Percent Load Transfer		0 Percent Load Transfer		100 Percent Load Transfer	
	Major (psi)	Minor (psi)	Major (psi)	Minor (psi)	Major (psi)	Minor (psi)	Major (psi)	Minor (psi)
Full	376	-237	391	-104	314	-262	343	-127
Partial	450	-413	501	-204	406	-634	508	-310

In view of the facts that load transfer is always provided in pavements and the critical stress always occurs when the load is far from the transverse joint, it is suggested that the edge stress, instead of the stress at the joint as recommended by PCA, be used for design of highway pavements. It is recognized that the old PCA design method based on the corner loading was used for a long time and gave reliable results. The current PCA method generally yields a critical stress comparable to that in the old method and therefore should also ensure a satisfactory service. However, the authors do not agree with PCA on the way in which this critical stress is obtained. When the outer face of the exterior tire is 2 ft from the pavement edge, designated by PCA as case I loading, the critical loading position is definitely not at the doweled joint but at a considerable distance from the joint. It is believed that comparable results could be obtained from the edge stress by placing the exterior tire a few inches from the edge. The use of edge stress for highway pavement design has the following advantages: It is in line with the use of interior stress for airport design because both assume that sufficient load transfer has reduced the stress at the joint to make it no longer critical; the edge stress is not affected significantly by the size of slab and the efficiency of load transfer at the transverse joint, so the influence chart developed by Pickett and Ray can still be used; lane width can be taken as a factor of design by specifying different distances between the outer tire and the pavement edge for various lane widths; and loss of subgrade contact at the pavement edge has less effect on edge stress than on stress at the joint, and the additional resultant edge stress can be more easily estimated.

CONCLUSIONS

A finite-element method programmed for a high-speed computer was developed for determining the stresses in concrete slabs with load transfer at the joints. The method is very efficient and checks closely with Westergaard's theoretical solutions as well as with those obtained from Pickett and Ray's influence chart. By the judicious selection of an appropriate k-value, it was found that the finite-element solutions also checked reasonably well with the stresses measured experimentally at the AASHO Road Test, thus verifying the validity of the method. Although a single k-value was used to compute the stresses for various slab thicknesses and axle loads, a comparison of the dynamic edge stresses clearly shows that under a given axle load the subgrade k-value should increase with the increase in slab thickness. This can be explained from the nonlinear behavior of subgrade soils because the thicker the slab is, the less the pressure on the subgrade is and the stiffer the soils are.

Numerical data are presented to illustrate the effect of loading position, efficiency of load transfer, and loss of subgrade contact on critical stresses. An analysis of the data results in the following conclusions:

1. In airport pavements, the most critical stress occurs when the load is in the interior of the slab. Stress due to loading at the joint can be kept smaller than the critical stress in the interior by use of load transfer devices having an efficiency of more than 70 percent at the joints.
2. In highway pavements with the outer face of the tire 2 ft from the edge, the most critical stress occurs when the load is at the transverse joint if no load transfer is provided, but at a considerable distance from the joint if load transfer is provided.
3. In highway pavements with the outer face of the tire adjacent to the edge and the slab in full contact with the subgrade, the most critical stress occurs when the load is at a considerable distance from the joint, regardless of the efficiency of load transfer.
4. In highway pavements with the outer tire adjacent to the edge and part of the slab not in contact with the subgrade, the most critical stress may occur at the transverse joint if no load transfer is provided. However, if load transfer is provided, the most critical stress occurs when the load is at a considerable distance from the joint.
5. In view of the fact that load transfer is always provided in pavements and the critical stress always occurs when the load is far from the transverse joint, it is suggested that the edge stress, instead of the stress at the joint as recommended by PCA, be used for the design of highway pavements.

ACKNOWLEDGMENTS

The study reported here was part of a faculty research program sponsored by the Department of Civil Engineering, University of Kentucky. The support given by the University of Kentucky Computing Center for use of an IBM 360 computer is appreciated.

REFERENCES

1. Westergaard, H. M. Stresses in Concrete Pavements Computed by Theoretical Analysis. Public Roads, April 1926, pp. 25-35.
2. Westergaard, H. M. Stress in Concrete Runways of Airports. HRB Proc., Vol. 19, 1939, pp. 197-202.
3. Westergaard, H. M. New Formulas for Stresses in Concrete Pavements of Airfields. Trans. ASCE, Vol. 113, 1948, pp. 425-444.
4. Pickett, G., and Ray, G. K. Influence Charts for Concrete Pavements. Trans. ASCE, Vol. 116, 1951, pp. 49-73.
5. Thickness Design for Concrete Pavements. Concrete Information, Portland Cement Assn., 1966.
6. Design of Concrete Airport Pavements. Portland Cement Assn., 1955.
7. Concrete Pavement Design for Roads and Streets Carrying All Classes of Traffic. Portland Cement Assn., 1951.
8. Hudson, W. R., and Matlock, H. Analysis of Discontinuous Orthotropic Pavement Slabs Subjected to Combined Loads. Highway Research Record 131, 1966, pp. 1-48.
9. Vesic, A. S., and Saxena, K. Analysis of Structural Behavior of AASHO Road Test Rigid Pavements. NCHRP Rept. 97, 1970.
10. Zienkiewicz, O. C., and Cheung, Y. K. The Finite Element Method in Structural and Continuum Mechanics. McGraw-Hill, 1967.
11. Cheung, Y. K., and Zienkiewicz, O. C. Plates and Tanks on Elastic Foundations: An Application of Finite Element Method. Internat. Jour. of Solids and Structures, Vol. 1, 1965, pp. 451-461.
12. Load Stresses at Pavement Edge, A Supplement to Thickness Design for Concrete Pavements. Concrete Information, Portland Cement Assn., 1969.
13. The AASHO Road Test: Report 5—Pavement Research. HRB Spec. Rept. 61E, 1962.
14. Teller, L. W., and Sutherland, E. C. The Structural Design of Concrete Pavements: Part 4—A Study of the Structural Action of Several Types of Transverse and Longitudinal Joint Designs. Public Roads, Vol. 17, 1936, pp. 143-171.